

Benchtop Experimental Studies of Stick-slip Mitigation Methods

Hilborn, H.

School of Mechanical Engineering, Georgia Institute of Technology, Atlanta, GA, United States Jorgenson, H.

University of South Florida, Tampa, FL, United States

Su, J.-C.

Sandia National Laboratories, Albuquerque, NM, United States

Mazumdar, A.

School of Mechanical Engineering, Georgia Institute of Technology, Atlanta, GA, United States

Copyright 2023 ARMA, American Rock Mechanics Association

This paper was prepared for presentation at the 57th US Rock Mechanics/Geomechanics Symposium held in Atlanta, Georgia, USA, 25–28 June 2023. This paper was selected for presentation at the symposium by an ARMA Technical Program Committee based on a technical and critical review of the paper by a minimum of two technical reviewers. The material, as presented, does not necessarily reflect any position of ARMA, its officers, or members. Electronic reproduction, distribution, or storage of any part of this paper for commercial purposes without the written consent of ARMA is prohibited. Permission to reproduce in print is restricted to an abstract of not more than 200 words; illustrations may not be copied. The abstract must contain conspicuous acknowledgement of where and by whom the paper was presented.

ABSTRACT: Drilling vibrations can cause inefficient drilling and accelerated damage to system components. Therefore, reducing or eliminating such vibrations is a major focus area for natural gas and geothermal drilling applications. One particularly important vibration mode is stick-slip. Stick-slip occurs when the bottom-hole angular velocity starts oscillating while the top-hole angular velocity remains relatively constant. This not only causes poor drilling, it is also difficult to detect using surface sensors. In this work, we describe the development and testing of a bench-top drilling system for studying stick-slip dynamics and mitigation. We show how this system can be used to produce stick-slip oscillations. Next, we use this data to formulate a data-driven rock-bit interaction model. This model can be combined with linear systems analysis to predict stick-slip and understand mitigation methods. We describe out instrumentation that enables closed-loop control under simulated communications constraints. We conclude by providing preliminary experimental data on bench-level stick-slip mitigation.

1 INTRODUCTION

Exploration via autonomous drilling processes for the exploitation of geothermal resources is an important focus area for drilling research. However, in order to fully realize the clean-energy promise of geothermal energy, key challenges still need to be resolved.

Issues arising in the drilling process often originate from a drill-string's increased susceptibility to vibrational oscillations, which grows as depths increase. Some examples of drilling vibrations include stick-slip, bit-bounce, and whirl. Torsional oscillations are the focus of this work.

Torsional vibrations result in a destructive phenomenon known as stick-slip. Initiated at the bit-rock surface, the drill-string bit experiences large angular velocity oscillations not seen at the surface Pavone and Desplans (1994).

Stick-slip results in premature bit wear and drill-string fracture.

Stick-slip is a fundamentally nonlinear and unpredictable phenomena. Stick-slip results from the combination of bit-rock interactions and drill-string compliance. As a result, there is a key need for experimental studies of stickslip dynamics and mitigation.

This work presents a scaled test-rig for experimental validation of stick-slip oscillation of a 2-DOF torsional system. This investigation contributes the following (1) the description of a bench-top experimental setup for evaluating stick-slip, (2) a data-driven rock-bit model that predicts stick-slip behavior, and (3) preliminary experimental results using closed-loop control with delayed bit information.

This paper is structured as follows. Section 3 provides a description of the bench-top test-rig. Sections 4 and 5 detail an overview of model dynamics, control system design and bench-top physical parameters as related to full-scale drill-string parameters. Section 6 summarizes initial experimental results which highlight the presence of stick-slip behaviors.

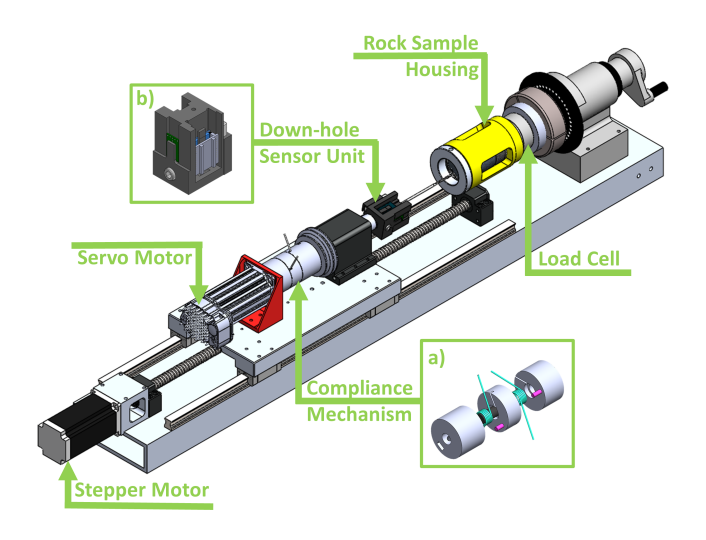


Fig. 1: Test Rig Overview.

2 BACKGROUND

2.1. Stick-Slip Oscillations

Authors have proposed many explanations for stick-slip. (Liu et al. (2014)) postulates the torsional mode being the dominant contributor causing drill-string damage and expediting failure. This can also provoke additional coupled instabilities (Yigit and Christoforou (1998)). Tang and Zhu (2020) found torsional vibrations are inclined to appear in deep-drilling scenarios, a very cost intensive process. Hance (2005) estimates that up to 56 percent of the cost variability of geothermal wells is linked to depth. This necessitates the development of models to efficiently augment geothermal drilling progress.

Analysis of torsional drill-string vibrations highlights how stick-slip occurs only when in contact with rock, whereas absent when lacking contact (Brett (1992)). This highlights the importance of including a bit-rock interaction model in when modeling stick-slip performance.

Previous works have developed varying non-linear friction models for bit-rock interaction contribution. Static friction models can be derived from the classical Coulomb friction model (Lin and Wang (1991); Jansen and van den Steen (1995)). Alternatively, Richard et al. (2004) utilizes

drag bit features, where the bit-rock interaction can be decomposed into cutting and frictional forces, where the cutting frictional net effect displays the important velocity-weakening effect (Kamel and Yigit (2014)). Besselink et al. (2011); Navarro-Lopez and Suarez (2004) use the velocity-weakening model, where a decrease in torque-on-bit(TOB) corresponds to increasing bit angular velocity with constant weight-on-bit (WOB).

Experiments can be used to collect data at the top of the drill-string. Finnie and Bailey (1960) observes coupling between longitudinal and torsional vibration, but there is no ability to observe down-hole conditions. Pavone and Desplans (1994); Jogi et al. (2002) performed further field experimentation, observing the stick-slip phenomenon with development of a down-hole measurement unit. This important work provided valuable data on stick-slip dynamics and mitigation methods. We leverage this past work in this paper.

Recent experimentation by Zhang et al. (2020) utilized a measurement tool to study down-hole behavior in a ultradeep well, where severe stick oscillations were generated. Field experimentation often utilizes existing drill sites, offers the greatest accuracy, but incurs high costs.

2.2. Laboratory Examination of Stick-Slip

Laboratory experimental analysis offers an intermediate solution, enabling rapid model validation and cost-effective experimentation. Brett (1992) demonstrated good correlation between laboratory and field experimentation. This shows that laboratory experimental systems have the potential to provide further insight into drill-string dynamic behavior. Laboratory tests can be performed frequently, under controlled conditions, and can utilize prototype hardware components.

Laboratory drilling systems commonly use a motor to command top-hole angular velocity. Real et al. (2018); Kovalyshen (2014); Khadisov et al. (2020) displays laboratory experiments implementing rock samples for drilling. Alternatively, Khulief and Al-Sulaiman (2009); ?); kat; Cayres et al. (2015) utilize braking mechanisms, friction and shaker plates in respective laboratory systems, stimulating drill-string vibrations in the absence of rock and cutting mechanisms. Sharma et al. (2020) presents an open-loop laboratory experimental setup, exploring crucial factors such as sensor quality and downhole sampling rate, resulting in the successful identification of stick-slip oscillations. Wiercigroch et al. (2017); Real et al. (2018); Mihajlović et al. (2004) laboratory setups utilize a slender rod to represent the drill-string in a minimized degree-offreedom(DOF) setup. Larger scale laboratory setups have also been explored in Xu et al. (2021) and Elsayed and

Aissi (2006), requiring a larger spacial footprint.

2.3. Stick-slip Mitigation using Feedback Control Many methods for controlling unwanted drill-string vibrations have been pursued. Passive methods (?Viguié et al. (2009)) involve... Active control methods have been frequently utilized to stabilize drilling vibrations(Brett (1992); Halsey et al. (1988); Serrarens et al. (1998); Yigit and Christoforou (2000); Christoforou and Yigit (2003)). It has been observed that increasing bit velocity and decreasing WOB(Jansen and van den Steen (1995); Pavone and Desplans (1994)) reduce the severity of stick-slip oscillations. However, due to the nonlinear friction relationship seen at the bit-rock surface, controller designs must be able to handle changing parameters resulting from bitrock nonlinearities. Losoya et al. (2018) implements control techniques for stick-slip stabilization in a labortory experimental test-rig. A key challenge in using closedloop control is associated with communicating down-hole information to the surface control system. An exciting method for high-speed communication involves wiredtelemetry. This enables high-speed, continuous data transmission. However, wired methods can fail due to drilling abrasions sustained in the drilling process, also incurring substantial installation and maintenance costs (Cheng and Tianhuai (2010)).

2.4. Communication Challenges

Wireless telemetry methods for drill-string measurementwhile-drilling (MWD) schemes commonly refers to mudpulse telemetry, extremely low frequency electromagnetic (EM) telemetry and acoustic telemetry. Commercially available technologies utilize mud-pulse telemetry, but suffers from multiple issues. Mud pulse telemetry uses mud pressure signal pulses that travel along the drilling pipe to deliver data to the surface, but at transmission speeds of $\sim 1500m/s$ Jaeger (2014). Additionally, mud-pulse suffers from relatively low transmission rates (approx. 10-40 bits/s) Berro and Reich (2019); ?); ?. Thus, mud-pulse telemetry is difficult to utilize in control schemes due to undesirable transmission characteristics. Similarly, EM telemetry can encounter undesirable high attenuation in specific drilling circumstances Schnitger and Macpherson (2009).

Acoustic telemetry Cheng and Tianhuai (2010) offers implementation advantages with theoretical transmission speeds 1-2 orders of magnitude over EM and mud-pulse telemetryXie et al. (2021). Acoustic telemetry was evaluated in field test programs, ?, meriting sufficient performance for commercial application. However, for deep drilled wells, the periodic nature of the drill-string structure causes exhibition of banded transmission characteris-

tics and surface signal degradation Sinanovic et al. (2004), resulting in installation of repeater systems for signal rectification. Shin (2021) shows promise in utilizing QPSK-modulation, enabling fast and accurate data transmission without the need for signal repeaters. Thus, the increased signal data transmission rate and increased signal reliability is favorable for control design schemes.

3 EXPERIMENTAL SYSTEM OVERVIEW

3.1. Physical System Description

An overview of the bench-top experimental system can be seen in Figure 1.The test-rig is comprised of (a) axial motion assembly, (b) torsional motion assembly, and (c) down-hole sensing assembly. The axial motion assembly consists of a stepper motor to drive linear motion via a lead screw. Torsional motion assembly consists of a DC motor simulating table-surface motion prescription to the drill-string. A 2-DOF drill-string is represented by a 3D printed mass-spring device, providing decreased system rigidity. As seen in Figure 1a, torsion springs are placed in series within a housing mechanism that limits angle displacement to the spring maximum of 120 degrees, aiding in increased system compliance over a rigid rod drillstring, better representing motion of a simulated lumped parameter drill-string models. The drill-string compliance mechanism furthermore translates motion down the drillstring via attachment to a lathe headstock, which holds a 1/8 inch carbide drillbit. Drilling occurs into 3 inch diameter Mancos Shale core, located in a custom core sample housing. The rock sample housing is placed in a rotating collet holder to rotate the shale core, maximizing the quantity of experiments to be performed per rock sample.

3.2. System Sensing

Displacement data acquisition is collected via a linear encoder attached to the drill-string frame. Down hole data acquisition occurs via a sensing unit attached to the drill-bit. This sensor module collects angular velocity data via a gyroscope, additionally housing an Arduino Pro Mini microcontoller, a Xbee antenna module for wireless data transmission back to the main computer, and a power source. Lastly, a load cell is attached to the rock core sample housing to obtain force and torque values. Acquired force values are utilized for WOB control. An overview of these processes can be viewed in Figure 2b. Instrumentation signaling and data acquisition is performed through a customized Labview interface. Experimentation occurs in two modes: manual feed mode or WOB-control mode.

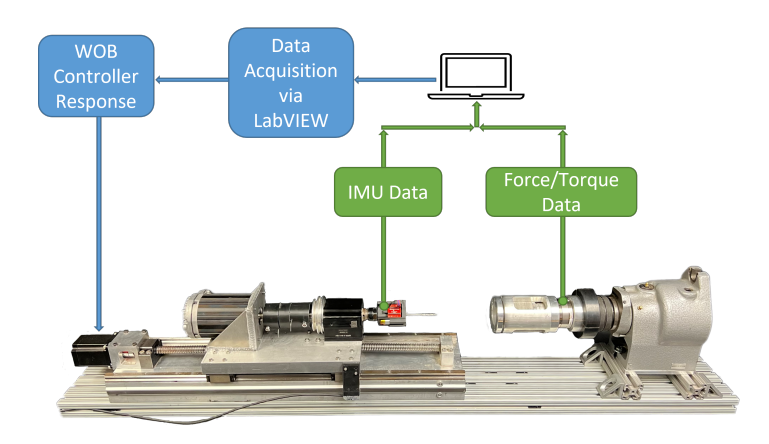


Fig. 2: Data Acquisition Process Flowchart.

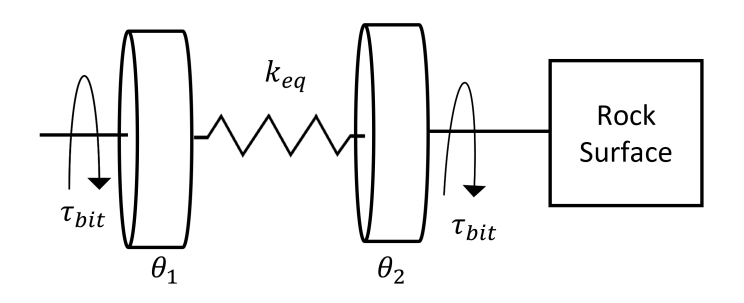


Fig. 3: 2-DOF Torsional drill-string Model.

4 LINEARIZED DRILL-STRING DYNAMIC MODEL

Utilizing the concept of similitude, replication of real-world drill-string parameters can be achieved in a laboratory system through scaling system attributes. We take the approach of replicating dynamic behavior of the system. This study utilizes lumped parameter representation of a 2-DOF electro-mechanical system, depicted in Figure 3. It is represented by the following model equations.

4.1. Mechanical System Dynamics

We approximate the surface drive for a drill as a speed-controlled motor. We assume that a closed-loop controller regulates the top hole speed (ω_1) automatically. In the case of this work, we use a stepper motor commanded with a constant frequency pulse train.

The key dynamics are therefore associated with the torsional spring and the motion of the bit. Many approximations for drill-strings use a 2-inertia lumped parameter model. In this work, we use the same type of approximation. However, in this case, this approximation is almost identical to our physical system. This is because we use a single torsional spring to emulate the drill string compliance.

The 2-DOF model can be defined by the following set of

dynamic equations:

$$\dot{\theta}_1 = \omega_1 \tag{1}$$

$$\dot{\omega}_1 = 0 \tag{2}$$

$$J_2\ddot{\theta}_2 + k_{eq}(\theta_2 - \theta_1) + c_2(\dot{\theta}_2 - \dot{\theta}_1) + \tau_b = 0$$
 (3)

 τ_b denotes the rock-bit friction torque at the drilling surface.

4.2. Rock-bit Interaction Dynamics

In this work we assume a rock-bit interaction model that is loosely based on that of ?. Specifically, this model assumes that the bit torque, τ_b is related to the weight on bit (WOB) raised to a power and the bit speed (ω_2) raised to a b.

$$\tau_b = \mu \cdot F_2^a \cdot \dot{\theta}_2^b \tag{4}$$

where F_2 represents downhole weight-on-bit, and $\dot{\theta}_2$ represents downhole angular velocity. An initial experimentation sweep was performed with the experimental test-rig to validate the velocity weakening frictional model referenced. The following bit-rock model coefficients were extracted ($\mu = 0.07$, a = 0.6, b = -0.49) via MATLAB curvefit toolbox, utilizing experimental data plotted in Figure 4.

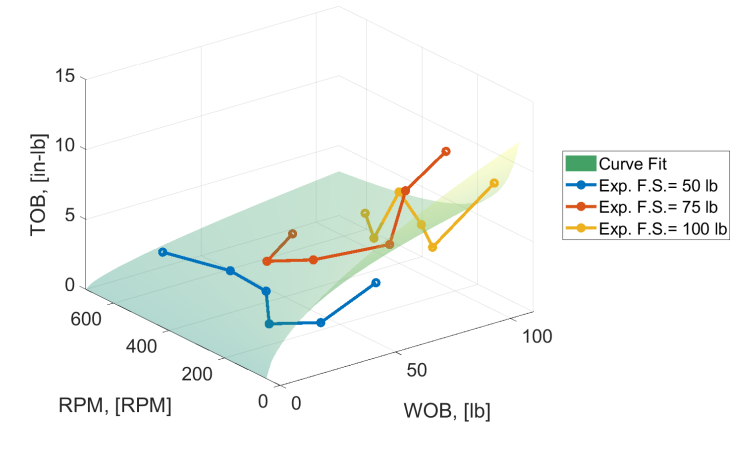


Fig. 4: Experimental Velocity Weakening Effect

To take near zero and negative speeds into account, bitrock contact smoothing was included. The inclusion of this continuity can be represented by Equation 5.

$$\tau_{b,s} = \tau_b \cdot (1 - e^{\frac{RPM}{RPM_0}}) \tag{5}$$

The coefficient RPM_0 is obtained via numerical simulation. A linearized version of the fitted bit-rock friction model is utilized for controller design. Although this does not fully capture the nonlinearities of the original friction

model, it captures a sufficient approximation around chosen WOB and angular velocity values. The linearization can be approximated as the following:

$$\tau_b \approx \tau_{b,0} + a_1 \Delta F_2 + a_2 \Delta \dot{\theta}_2 \tag{6}$$

$$a_1 = 0.6\gamma \omega_{2.0}^{-0.49} F_{2.0}^{-0.4} \tag{7}$$

$$a_2 = -0.49\gamma F_{2.0}^{0.6} \omega_{2.0}^{-1.49} \tag{8}$$

where ΔF_2 and $\Delta \dot{\theta}_2$ are operational conditions which our system is linearized about. Using frequency domain analysis tools, in tandem with our linearized rock bit interaction model, we can generate our system plant model as the following:

$$G_p(s) = \frac{\Delta \dot{\theta}_2(s)}{\Delta F_2(s)} = \frac{-a_1 s}{J_2 s^2 + a_2 s + B_2 s + K_c}$$
(9)

The system output is down-hole angular velocity, and the input is surface table force.

4.3. Communication Dynamics

Under open loop conditions, the plant poles will always lie in the right-hand side of the imaginary axis, representing inherent system instability. Implementing feedback control occurs with the inclusion of down-hole state data, to update surface level input accordingly. Field drill-string operations perform real time data transmission using mudpulse telemetry. This wireless telemetry communication method transmits data utilizing pressure wave propagation. As shown in Mwachaka et al. (2019), due to lower attenuation at greater depths, low data rates using simple modulation schemes are commonly used. These telemetry methods often suffer from added noise; this model neglects noise, and assumes 2 8-bit numbers are needed from the down-hole sensing system($\dot{\theta}_2$, $\ddot{\theta}_2$).

We can simplify communication dynamics with the following model assumptions.

The first element of wireless communication (low data rates) can be modeled as a pure delay combined with a zero-order-hold (ZOH), assumed to be held at a fixed period T.

$$G_{ZOH}(s) = \frac{1 - e^{-Ts}}{Ts} \tag{10}$$

Next, we account for a pure transmission delay (Eq. 11). This is produced from the phenomenon of speed of sound traveling through surrounding terrain, a term associated with the length of the drill-string.

$$G_{delay}(s) = e^{-t_{delay}s} \tag{11}$$

A pure time delay, however, cannot be represented in transfer function notation. We approximate with 2^{nd} order Pade' approximation (Eq. 12), used to provide greater approximation accuracy.

$$e^{-as} \approx \frac{a^2s^2 - 6as + 12}{a^2s^2 + 6as + 12} \tag{12}$$

This can be used to create transfer functions for both the ZOH and the pure delay.

$$G_s(s) = \frac{\omega_{2,meas}(s)}{\omega_1(s)} = G_{ZOH}(s)G_{delay}(s)$$
(13)

where

$$G_{ZOH}(s) \approx \frac{12}{T^2 s^2 + 6T s + 12}$$
 (14)

$$G_{delay}(s) \approx \frac{t_{delay}^2 s^2 - 6t_{delay} s + 12}{t_{delay}^2 s^2 + 6t_{delay} s + 12}$$
(15)

The overall loop transmission function can be modeled as follows.

$$G_{loop}(s) = G_s(s) \cdot G_p(s) \tag{16}$$

For the following simulations, the corresponding simulated versus physical system parameters can seen in Table 1. Values for t_{delay} correspond to a physical drill-string of 3000 meters in depth.

Table 1: drill-string Model Parameters.

Parameter	Simulated	Experimental
k_{th} (Nm·rad ⁻¹)	386.6	0.1772
ω_n [Hz]	1.480	0.7074
$J_2 (kg \cdot m^2)$	617.6	0.7083
t_{delay}	0.5172	0.5172
T	0.25	0.25

5 CONTROL DESIGN AND STABILITY ANALYSIS

5.1. Control Architecture

Passive methods such as adding friction via down-hole tools or drill-bit designs are set of techniques for drill-string stabilization. However the design and performance of passive mechanisms may be environment-specific, and certain drilling conditions may still elicit instabilities.

Active feedback control methods are an alternative approach to achieving system stability. By using feedback of system-states, the closed loop poles can be moved to the stable region of the complex plane. One method utilized is using the top-hole force to increase WOB in response to

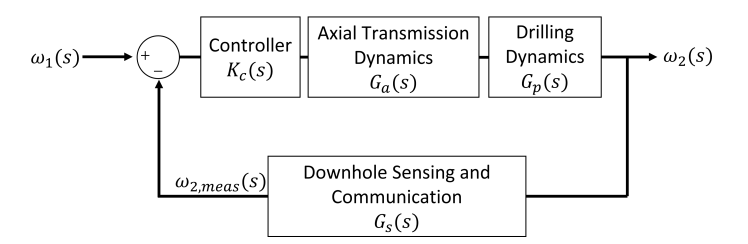


Fig. 5: System Block Diagram.

differences between the top and bottom hole rotation rates Pavone and Desplans (1994); Navarro-Lopez and Suarez (2004).

A controller of the following architecture was used.

$$\Delta F_1(s) = K_c(s)(\omega_1(s) - \omega_{2,meas}(s)) \tag{17}$$

This structure is illustrated in the block diagram shown in Fig. 5. The closed loop transfer function, G_{CL} is shown below.

$$G_{CL}(s) = \frac{K_c(s)G_p(s)}{1 + K_c(s)G_p(s)G_s(s)}$$
(18)

We use $K_c(s)$ to refer to a generic frequency domain controller. For the scope of this work, we focus on a proportional-plus-derivative (PD) controller. This architecture is shown in Eq. 19. In this formulation, K represents the loop gain while z_c represents the controller's zero location, evaluated at $z_c = 0.5$.

$$K_C(s) = K(s + z_C) \tag{19}$$

Frequency-domain analysis is utilized for controller design. The benchtop system loop transfer function is comprised only of the plant, controller, and zero-orderhold. Nyquist analysis is used to evaluate phase at crossover frequencies, such that we may manipulate loop gain, K, for desired frequency cross over points that maintain closed-loop stability.

5.2. Controller Simulated Validation

Utilizing parameters from Table 1, controller design can be rapidly simulated, modify the bench-top drill-string testbed until we successfully emulate system dynamics similar to physical drill-string parameters. In Fig. 6, field and laboratory experimental responses are shown in the frequency domain. With analogous responses recorded, we may then use these parameters to manipulate the loop gain value until crossover frequencies indicate a stabilized frequency response. Results of controller design with targeted gain margin values may be seen in 7. Corresponding time domain results are exhibited in Fig. 8.

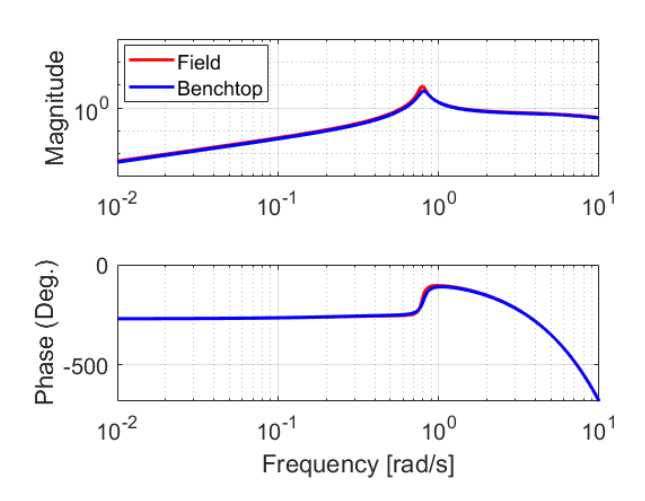


Fig. 6: Field vs. Benchtop Parameters, Frequency Response

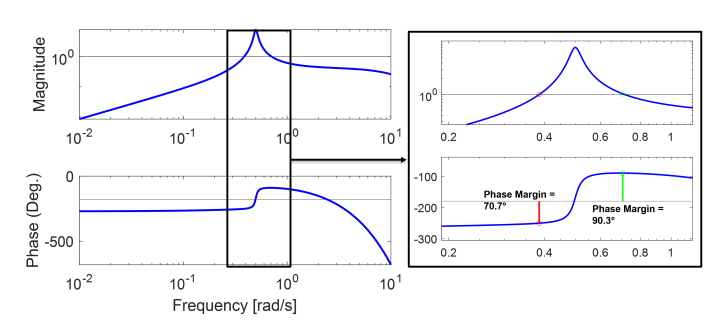


Fig. 7: System Frequency Response: Loop

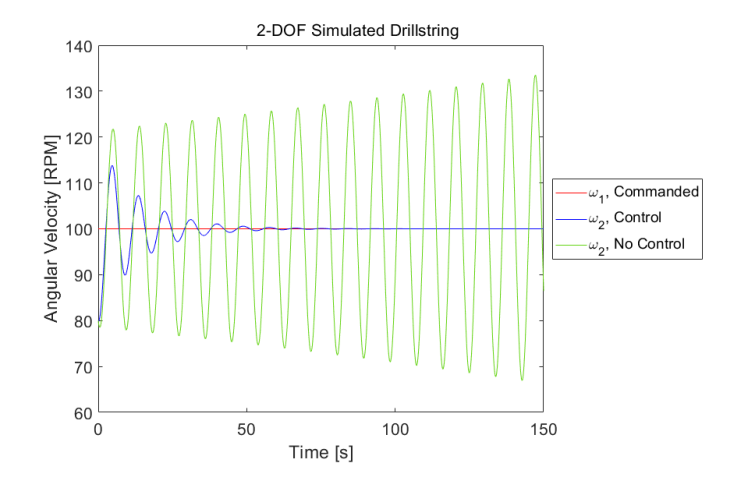


Fig. 8: Simulated No WOB Control vs PD Control.

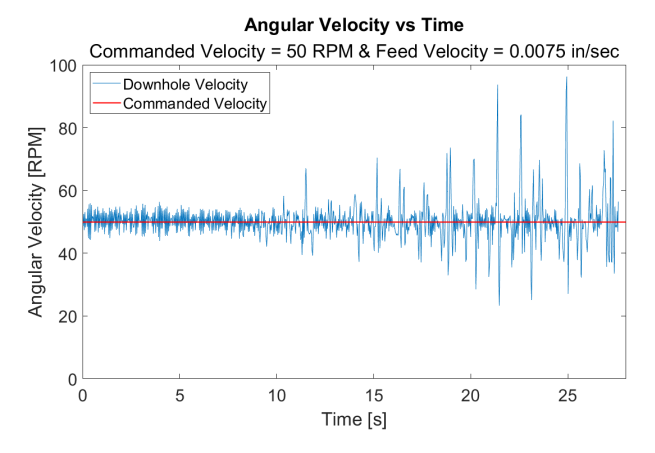


Fig. 9: Experimental Result: Example Benchtop stick-slip Replication in Constant Feed Mode.

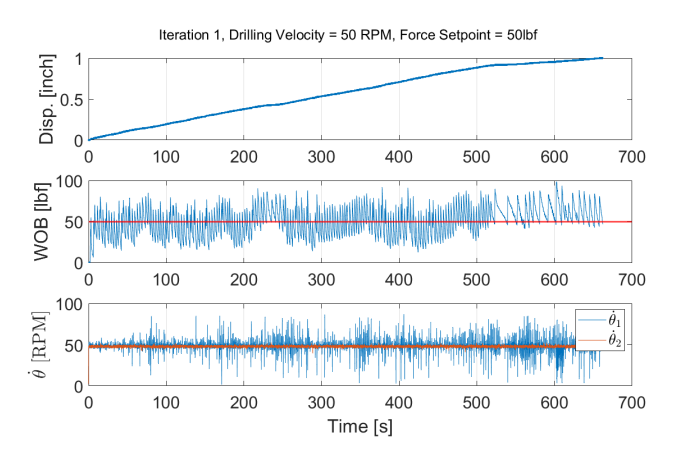


Fig. 10: Experimental Result: WOB Control, stick-slip present.

6 EXPERIMENTAL RESULTS

6.1. Characteristic Torsional Vibrations

Primary drilling experimentation demonstrates system open-loop behavior. Figure 9 displays the presence of stick-slip in the time domain, amplifying as experimentation occurs. Literature suggests stick-slip is amplified at lower drilling angular velocities and higher WOB values. Control implementation on the bench top test setup confirmed the presence of stick-slip at these conditions. Time domain results of experimentation at varying WOB setpoints are shown in Figures 11 and 10. Sustained oscillations are observed in Figure 10, amplified from approximately t=40 to 65, where nominal torsional oscillations only are seen in Figure 11 for the entire duration of the experiment.

ADD.....

Closed-loop controller implementation validation was performed with the parameters included in Table 2, also denoting achievement of respective performance metrics:

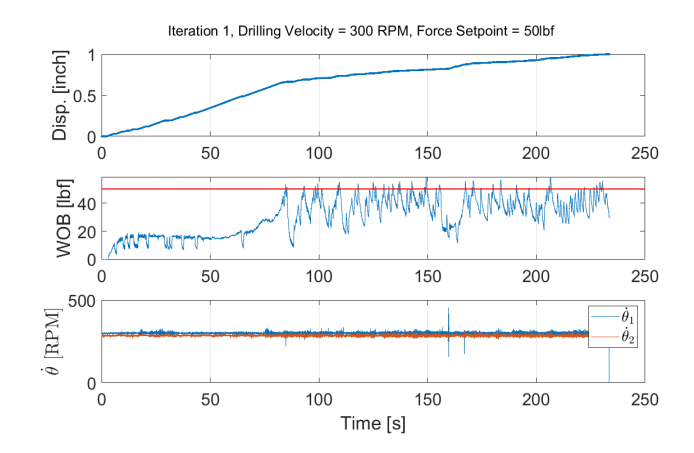


Fig. 11: Experimental Result: WOB Control, No stick-slip present.

Table 2: PID Controller Characteristics.

Parameter	Value
Proportional Gain (Ns/rad)	-195
Rise Time (s)	1.98
Overshoot (%)	38.19

7 CONCLUSIONS

This work presents preliminary results of a simplified benchtop experimental system for ready modulation and analysis of drill-string dynamics.

With a torsional-spring loaded drill-string device, driven by a tophole motor, shale rock samples are drilled. A downhole measurement device measures angular velocity at the rock surface; a load cell collects WOB and TOB data elicited from the drilling process. Additionally, a WOB control system was implemented, mitigating stickslip with decreased WOB values.

ACKNOWLEDGMENTS

This paper describes objective technical results and analysis. Any subjective views or opinions that might be expressed in the paper do not necessarily represent the views of the U.S. Department of Energy or the United States Government. Sandia National Laboratories is a multimission laboratory managed and operated by National Technology & Engineering Solutions of Sandia, LLC, a wholly owned subsidiary of Honeywell International Inc., for the U.S. Department of Energy's National Nuclear Security Administration under contract DE-NA0003525.

REFERENCES

1. Experimental Investigation of the Stick-Slip Phenomena of the Drill Pipe. St. Johnâs, Newfoundland, Canada.

- Berro, M. J. and Reich, M. (2019). Laboratory investigations of a hybrid mud pulse telemetry (HMPT)-A new approach for speeding up the transmitting of MWD/LWD data in deep boreholes. *Journal of Petroleum Science and Engineering*, 183:106374.
- 3. Besselink, B., van de Wouw, N., and Nijmeijer, H. (2011). A Semi-Analytical Study of Stick-Slip Oscillations in Drilling Systems. *Journal of Computational and Nonlinear Dynamics*, 6(2):021006.
- 4. Brett, J. (1992). The genesis of torsional drillstring vibrations. *SPE Drilling Engineering*, 7(3):168 â 174.
- Cayres, B., da Fonseca, C., Santos, A., and Weber, H. I. (2015). Analysis of Dry Friction-Induced Stick-Slip in an Experimental Test Rig Modeling a Drill String. In Pennacchi, P., editor, *Proceedings of the 9th IFToMM International Conference on Rotor Dynamics*, volume 21, pages 195–204. Springer International Publishing, Cham. Series Title: Mechanisms and Machine Science.
- Cheng, L. and Tianhuai, D. (2010). Signal wireless transmission behaviors along the drillstring using extensional stress waves. In 2010 IEEE International Conference on Intelligent Computing and Intelligent Systems, volume 2, pages 541–545.
- Christoforou, A. and Yigit, A. (2003). Fully coupled vibrations of actively controlled drillstrings. *Journal of Sound and Vibration*, 267(5):1029–1045.
- 8. Elsayed, M. A. and Aissi, C. (2006). Analysis of Shock Absorber Characteristics for Drillstrings. In *Volume 3: Dynamic Systems and Controls, Symposium on Design and Analysis of Advanced Structures, and Tribology*, pages 93–101, Torino, Italy. ASMEDC.
- Finnie, I. and Bailey, J. J. (1960). An Experimental Study of Drill-String Vibration. *Journal of Engineering for Industry*, 82(2):129–135.
- Halsey, G., Kyllingstad, A., and Kylling, A. (1988). Torque Feedback Used to Cure Slip-Stick Motion. volume All Days of SPE Annual Technical Conference and Exhibition. SPE-18049-MS.
- 11. Hance, C. N. (2005). Factors Affecting Costs of Geothermal Power Development.
- 12. Jaeger, F. (2014). Experimental study: Measurement of sonic speed of drilling muds under shear stress. Technical report, IBJ Technology, Markkleeberg, DE.
- 13. Jansen, J. and van den Steen, L. (1995). Active damping of self-excited torsional vibrations in oil well drillstrings. *Journal of Sound and Vibration*, 179(4):647–668.
- Jogi, P. N., Macpherson, J. D., and Neubert, M. (2002). Field Verification of Model-Derived Natural Frequencies of a Drill String. *Journal of Energy Resources Technology*, 124(3):154–162.
- 15. Kamel, J. M. and Yigit, A. S. (2014). Modeling and analysis of stick-slip and bit bounce in oil well drillstrings equipped with drag bits. *Journal of Sound and Vibration*, 333(25):6885–6899.
- Khadisov, M., Hagen, H., Jakobsen, A., and Sui, D. (2020).
 Developments and experimental tests on a laboratory-scale drilling automation system. *Journal of Petroleum Explo*ration and Production Technology, 10(2):605–621.
- 17. Khulief, Y. A. and Al-Sulaiman, F. A. (2009). Laboratory investigation of drillstring vibrations. *Proceedings of the*

- Institution of Mechanical Engineers, Part C: Journal of Mechanical Engineering Science, 223(10):2249–2262.
- Kovalyshen, Y. (2014). Experiments on Stick-Slip Vibrations in Drilling with Drag Bits. volume All Days of U.S. Rock Mechanics/Geomechanics Symposium. ARMA-2014-7108.
- Lin, Y.-Q. and Wang, Y.-H. (1991). Stick-Slip Vibration of Drill Strings. *Journal of Engineering for Industry*, 113(1):38–43.
- Liu, X., Vlajic, N., Long, X., Meng, G., and Balachandran,
 B. (2014). State-Dependent Delay Influenced Drill-String Oscillations and Stability Analysis. *Journal of Vibration and Acoustics*, 136(5).
- Losoya, E. Z., Gildin, E., and Noynaert, S. F. (2018). Realtime Rate of Penetration Optimization of an Autonomous Lab-Scale Rig using a Scheduled-Gain PID Controller and Mechanical Specific Energy. *IFAC-PapersOnLine*, 51(8):56–61.
- Mihajlović, N., van Veggel, A. A., van de Wouw, N., and Nijmeijer, H. (2004). Analysis of Friction-Induced Limit Cycling in an Experimental Drill-String System. *Journal of Dynamic Systems, Measurement, and Control*, 126(4):709–720.
- 23. Mwachaka, S. M., Wu, A., and Fu, Q. (2019). A review of mud pulse telemetry signal impairments modeling and suppression methods. *Journal of Petroleum Exploration and Production Technology*, 9(1):779–792.
- 24. Navarro-Lopez, E. and Suarez, R. (2004). Practical approach to modelling and controlling stick-slip oscillations in oilwell drillstrings. In *Proceedings of the 2004 IEEE International Conference on Control Applications*, 2004., volume 2, pages 1454–1460, Taipei, Taiwan. IEEE.
- 25. Pavone, D. and Desplans, J. (1994). Application of High Sampling Rate Downhole Measurements for Analysis and Cure of Stick-Slip in Drilling. All Days. SPE-28324-MS.
- Real, F., Lobo, D., Ritto, T., and Pinto, F. (2018). Experimental analysis of stick-slip in drilling dynamics in a laboratory test-rig. *Journal of Petroleum Science and Engineering*, 170:755–762.
- Richard, T., Germay, C., and Detournay, E. (2004). Self-excited stickâslip oscillations of drill bits. *Comptes Rendus Mécanique*, 332(8):619–626.
- 28. Schnitger, J. and Macpherson, J. (2009). Signal Attenuation for Electromagnetic Telemetry Systems. volume All Days of *SPE/IADC Drilling Conference and Exhibition*. SPE-118872-MS.
- 29. Serrarens, A., Van De Molengraft, M., Kok, J., and Van Den Steen, L. (1998). Hâ control for suppressing stick-slip in oil well drillstrings. *IEEE Control Systems*, 18(2):19 â 30.
- 30. Sharma, A., Srivastava, S., and Teodoriu, C. (2020). Experimental design, instrumentation, and testing of a laboratory-scale test rig for torsional vibrationsathe next generation. *Energies*, 13(18).
- 31. Shin, Y. (2021). Simulation of QPSK-based acoustic telemetry through drillstring. *Journal of Mechanical Science and Technology*, 35(3):963–971.
- 32. Sinanovic, S., Johnson, D., Shah, V., and Gardner, W. (2004). Data communication along the drill string using acoustic waves. volume 4, pages iv 909.

- 33. Tang, L. and Zhu, X. (2020). Effects of Drill String Length on Stick-Slip Oscillation of the Oilwell Drill String. *Iranian Journal of Science and Technology, Transactions of Mechanical Engineering*, 44(2):497–506.
- 34. Viguié, R., Kerschen, G., Golinval, J. C., McFarland, D. M., Bergman, L. A., Vakakis, A. F., and van de Wouw, N. (2009). Using Targeted Energy Transfer to Stabilize Drillstring Systems. page 12.
- 35. Wiercigroch, M., Nandakumar, K., Pei, L., Kapitaniak, M., and Vaziri, V. (2017). State dependent delayed drill-string vibration: Theory, experiments and new model. *Procedia IUTAM*, 22:39–50. IUTAM Symposium on Nonlinear and Delayed Dynamics of Mechatronic Systems.
- Xie, H., Zhang, P., and Zhou, J. (2021). Numerical study of drill string uncertainty in acoustic information transmission. *IOP Conference Series: Earth and Environmental Science*, 734(1):012024.
- 37. Xu, Y., Zhang, H., and Guan, Z. (2021). Dynamic Characteristics of Downhole Bit Load and Analysis of Conversion Efficiency of Drill String Vibration Energy. *Energies*, 14(1):229.
- 38. Yigit, A. and Christoforou, A. (1998). Coupled Torsional and Bending Vibrations of Drillstrings Subject to Impact with Friction. *Journal of Sound and Vibration*, 215(1):167–181.
- 39. Yigit, A. and Christoforou, A. (2000). Coupled torsional and bending vibrations of actively controlled drillstrings. *Journal of Sound and Vibration*, 234(1):67–83.
- Zhang, H., Di, Q., Li, N., Wang, W., and Chen, F. (2020). Measurement and simulation of nonlinear drillstring stickâslip and whirling vibrations. *International Journal of Non-Linear Mechanics*, 125:103528.